Journal of Molecular Spectroscopy 318 (2015) 26–33

Contents lists available at ScienceDirect

Journal of Molecular Spectroscopy

journal homepage: www.elsevier.com/locate/jms

High resolution FTIR study of $^{34}S^{16}O_2$: The bands $2\nu_3$, $2\nu_1+\nu_2$ and $2\nu_1+\nu_2-\nu_2$

O.N. Ulenikov [a,b,*], O.V. Gromova [a], E.S. Bekhtereva [a,b], Yu.V. Krivchikova [a], E.A. Sklyarova [a], T. Buttersack [c], C. Sydow [c], S. Bauerecker [c]

[a] Institute of Physics and Technology, National Research Tomsk Polytechnic University, Tomsk 634050, Russia
[b] National Research Tomsk State University, Tomsk 634050, Russia
[c] Institut für Physikalische und Theoretische Chemie, Technische Universität Braunschweig, D-38106 Braunschweig, Germany

ARTICLE INFO

Article history:
Received 25 August 2015
In revised form 24 September 2015
Accepted 25 September 2015
Available online 3 October 2015

Keywords:
$^{34}SO_2$ sulfur dioxide
High-resolution spectra
Spectroscopic parameters

ABSTRACT

The high resolution infrared spectrum of the $^{34}S^{16}O_2$ molecule was recorded in the region of 2600–2810 cm^{-1} where the strong $2\nu_3$ band is located. About 2500 transitions with maximum values of quantum numbers $J^{max.}=76$ and $K_a^{max.}=26$ were assigned to the $2\nu_3$ band. The very weak $2\nu_1+\nu_2$ band was recorded and analyzed for the first time. This gave us the possibility to find and analyze, for the first time, the hot band $2\nu_1+\nu_2-\nu_2$, which is located in the 2200–2380 cm^{-1} region and totally covered by the strong $2\nu_1$ band. In general, about 1370 transitions were assigned to the bands $2\nu_1+\nu_2$ and $2\nu_1+\nu_2-\nu_2$, and 302 ro-vibrational energies of the (210) state were determined. Ro-vibrational energies obtained from experimental data for both the (002), and (210) vibrational states were used in the weighted list square fit of the parameters of the effective Hamiltonian, which takes into account additional interactions with the (130) and (050) vibrational states. The set of parameters obtained from the fit reproduces the initial experimental data with accuracies close to experimental uncertainties.

1. Introduction

In this paper we continue our recent work, Refs. [1–6], of the analysis of high resolution rotation–vibration spectra of sulfur dioxide, which is an important substance in many fields of study of the universe, such as chemistry, interstellar space, planetary nebulae, study of atmospheres of the Earth and Venus, food technology, and many others (see, e.g., Refs. [7–15]). For this reason, numerous spectroscopic studies of the sulfur dioxide molecule have been made during many years as well in the microwave, submillimeter wave and infrared regions (extensive list of references to earlier studies of sulfur dioxide spectra can be found, e.g., in Ref. [16]).

The present study focuses on the spectroscopic analysis of the $^{34}S^{16}O_2$ isotopologue of sulfur dioxide which is the naturally mostly abundant (natural abundance is about 4% species of sulfur dioxide) and most intensively studied species after $^{34}S^{16}O_2$. The high resolution spectra of $^{34}S^{16}O_2$ have been analyzed both in the microwave (see, e.g., Refs. [17–19]) and infrared (IR), Refs. [20–27], regions. The goal of the present study is an analysis of the 2600–2810 cm^{-1} spectral region, where the strong $2\nu_3$ band is located. Earlier this band was discussed in Ref. [22] (see also Table 1, where statistical information about bands considered in this paper is presented). In the present investigation, we were able not only to increase information about earlier analyzed $2\nu_3$ band, but also, for the first time, to assign about 770 transitions to the weak $2\nu_1+\nu_2$ band. In turn, this gave us the possibility to find, for the first time, also the hot $2\nu_1+\nu_2-\nu_2$ band, which is located in the 2200–2380 cm^{-1} region and totally covered by the strong $2\nu_1$ band. The experimental spectrum and corresponding experimental details are presented in Section 2. Section 3 gives briefly the theoretical background for description of experimental data. The results of analysis of the experimental data are discussed in Section 4.

2. Experimental details

The $^{34}SO_2$ sample was generated by controlled combustion of ^{34}S which was purchased from Sigma–Aldrich with a purity of 90 atom % (99% abundance of $^{34}SO_2$ in the sample). The generation procedure was described in detail in our preceding papers [28,29] and especially [30]. For the present analysis two spectra of the spectral region of 1800–3640 cm^{-1} have been exploited;

* Corresponding author at: Institute of Physics and Technology, National Research Tomsk Polytechnic University, Tomsk 634050, Russia.
E-mail address: Ulenikov@mail.ru (O.N. Ulenikov).

http://dx.doi.org/10.1016/j.jms.2015.09.009
0022-2852/

Table 1
Statistical information for the $2\nu_3$, $2\nu_1+\nu_2$, and $2\nu_1+\nu_2-\nu_2$ bands of $^{34}S^{16}O_2$.

Band	Center/cm^{-1}	J^{max}	K_a^{max}	N_{tr}[a]	N_l[b]	m_1[c]	m_2[c]	m_3[c]
1	2	3	4	5	6	7	8	9
$2\nu_3$, Ref. [22]	2679.8009	57	18		488	36.5	28.3	35.2
$2\nu_3$, this work	2679.7998	76	26	2500	830	84.6	10.1	5.3
$2\nu_1+\nu_2$, this work	2788.6387	45	11	770	302[d]	29.5[d]	30.9[d]	39.6[d]
$2\nu_1+\nu_2-\nu_2$, this work	2275.1000	43	13	600	302[d]	29.5[d]	30.9[d]	39.6[d]

[a] N_{tr} is the number of assigned transitions.
[b] N_l is the number of obtained upper-state energies.
[c] Here $m_i = n_i/N_l \times 100\%$ (i = 1, 2, 3); n_1, n_2, and n_3 are the numbers of upper-state energies for which the differences $\delta = E^{exp} - E^{calc}$ satisfy the conditions $\delta \leqslant 2\times10^{-4}$ cm^{-1}, 2×10^{-4} cm$^{-1} < \delta \leqslant 4\times10^{-4}$ cm^{-1}, and $\delta > 4\times10^{-4}$ cm^{-1}.
[d] Obtained on the basis of data for the $2\nu_1+\nu_2$ and $2\nu_1+\nu_2-\nu_2$ bands.

an overview of the experimental conditions is given in Table 2. A tungsten IR radiation source, a CaF_2 beamsplitter, an indium-antimonide (InSb) semiconductor detector and KBr windows have been used. The optical resolution was 0.0025 and 0.003 cm^{-1}, defined by $1/d_{MOPD}$ (maximum optical path difference). In combination with the weak Norton–Beer apodization this leads to an instrumental resolution of 0.002 cm^{-1}. The Doppler broadening for $^{34}S^{16}O_2$ at 298.15 K was between 0.0033 cm^{-1} (at 2200 cm^{-1}) and 0.0043 cm^{-1} (at 2810 cm^{-1}). The pressure broadening was about 0.0016 cm^{-1} at the used pressure of 480 Pa which means that it has to be considered. So the total line width results between 0.0042 and 0.0052 cm^{-1} (root sum square approximation of convolution) in accordance with the experimental results. The spectral line calibration was performed with N_2O lines at a partial N_2O pressure of about 10 Pa and with water lines (in one spectrum). The total recording time was between 32 and 49 h for 810 scans and 1480 scans.

3. Theoretical background

Because $^{34}S^{16}O_2$ is an asymmetric top molecule with the asymmetry parameter $\kappa = (2B-A-C)/(A-C) \simeq -0.939$, its vibrational modes q_1 and q_2 are symmetric, and the third vibrational mode, q_3, is antisymmetric. As the consequence, both the (002) and the (210) vibrational states which are considered in the present study, are symmetric, and all corresponding bands, $2\nu_3$, $2\nu_1+\nu_2$ and $2\nu_1+\nu_2-\nu_2$, are of b-type. For such band types the following selection rules are valid (see, e.g., Refs. [31–33]):

$$\Delta J = 0,\pm1, \quad \Delta K_a = odd, \quad \Delta K_c = odd.$$

In the present study we followed a fact which is well known in the literature (see, *e.g.*, Ref. [25]), namely that the ro-vibrational states $[JK_aK_c]$ of $(\nu_1\nu_2\nu_3)$ of SO_2, on the one hand, and $[JK_a \pm 2K_c \mp 2]$ of $(\nu_1 \pm 1\,\nu_2 \mp 2\,\nu_3)$, on the other hand, can strongly interact with each others for the values of quantum number K_a between 12 and 14. This means, that in the present study it is reasonable to take into account the Fermi type interactions between the states (210), (130), and (050). As the analysis showed, it is possible to skip Coriolis type interactions in our study (we did not recognize local perturbations caused by the Coriolis interaction in our experimental spectra). Additionally, as the estimation showed, which was made on the basis of the results of the isotopic substitution theory, Refs. [34–36], and the general properties of the vibration–rotation Hamiltonian (see, e.g., Refs. [37–39]), there is only 5.5 cm^{-1} difference between the vibrational energies of the vibrational states (002) and (130). It means, that local resonance interactions between ro-vibrational states of (002) and (130) are expected in spite of the large value of the $\Delta v = 6$ ($\Delta v = |\Delta v_1| + |\Delta v_2| + |\Delta v_3|$) difference. In consequence, for the theoretical analysis of our experimental data the Hamiltonian model in the following form was used:

$$H^{vib.-rot.} = \sum_{v,\tilde{v}} |v\rangle\langle\tilde{v}|H^{v\tilde{v}}, \tag{1}$$

where v and $\tilde{v}$ denote interacting vibrational states, and the summation extends over four vibrational states: $|1\rangle \equiv (002, A_1)$, $|2\rangle \equiv (210, A_1)$, $|3\rangle \equiv (130, A_1)$, and $|4\rangle \equiv (050, A_1)$. In this model the diagonal block operators are the traditional Watson type operators in A reduction and I^r representation [40–42],

$$\begin{aligned} H^{vv} = {} & E^v + \left[A^v - \frac{1}{2}(B^v + C^v)\right]J_z^2 + \frac{1}{2}(B^v + C^v)J^2 + \frac{1}{2}(B^v \\ & - C^v)J_{xy}^2 - \Delta_K^v J_z^4 - \Delta_{JK}^v J_z^2 J^2 - \Delta_J^v J^4 - \delta_K^v [J_z^2, J_{xy}^2]_+ - 2\delta_J^v J^2 J_{xy}^2 \\ & + H_K^v J_z^6 + H_{KJ}^v J_z^4 J^2 + H_{JK}^v J_z^2 J^4 + H_J^v J^6 \\ & + [h_K^v J_z^4 + h_{JK}^v J_z^2 J^2 + h_J^v J^4, J_{xy}^2]_+ + L_K^v J_z^8 + L_{KKJ}^v J_z^6 J^2 + L_{JK}^v J_z^4 J^4 \\ & + L_{JJK}^v J_z^2 J^6 + L_J^v J^8 + [l_K^v J_z^6 + l_{KJ}^v J_z^4 J^2 + l_{JK}^v J_z^2 J^4 + l_J^v J^6, J_{xy}^2]_+ \\ & + P_K^v J_z^{10} + P_{KKKJ}^v J_z^8 J^2 + P_{KKJ}^v J_z^6 J^4 + \cdots \end{aligned} \tag{2}$$

In Eq. (2), J_α ($\alpha = x, y, z$) are the components of the angular momentum operator defined in the molecule-fixed coordinate system, $J_{xy}^2 = J_x^2 - J_y^2$, and $[\ldots,\ldots]_+$ denotes an anticommutator. Because of the symmetry properties of the $^{34}S^{16}O_2$ molecule, the nondiagonal block operators can be of two types: Coriolis interactions of the B_1-symmetry and Fermi interactions. However, in accordance with the above said, in the present study we took into account only the Fermi-type interactions which are described by the following operators (see, e.g., Refs. [43,44])

$$\begin{aligned} H_{v\tilde{v}} = {} & {}^{v\tilde{v}}F_0 + {}^{v\tilde{v}}F_K J_z^2 + {}^{v\tilde{v}}F_J J^2 + {}^{v\tilde{v}}F_{KK} J_z^4 + {}^{v\tilde{v}}F_{KJ} J_z^2 J^2 + {}^{v\tilde{v}}F_{JJ} J^4 \\ & + \ldots + {}^{v\tilde{v}}F_{xy}(J_x^2 - J_y^2) + {}^{v\tilde{v}}F_{Kxy}\{J_z^2, (J_x^2 - J_y^2)\}_+ \\ & + 2\,{}^{v\tilde{v}}F_{Jxy} J^2 (J_x^2 - J_y^2) + {}^{v\tilde{v}}F_{KKxy}\{J_z^4, (J_x^2 - J_y^2)\}_+ + \cdots \end{aligned} \tag{3}$$

Table 2
Experimental setup for the studied bands of $^{34}S^{16}O_2$.

Spectr.	Region/cm^{-1}	Resolution/cm^{-1}	Measuring time/h	No. of scans	Source	Detector	Beam-splitter	Opt. path-length/m	Aperture/mm	Temp./°C	Pressure/Pa	Calibr. gas
I	1800–2800	0.0025	32	810	Tungsten	InSb	CaF_2	24.0	1.15	23 ± 0.5	480	N_2O
II	2580–3640	0.0030	49	1480	Tungsten	InSb	CaF_2	24.0	1.15	23 ± 0.5	480	N_2O, H_2O

4. Assignment of transitions and analysis of the results

The survey spectrum in the region of 2600–2810 cm^{-1}, where the strong $2\nu_3$ and very weak $2\nu_1+\nu_2$ bands of $^{34}S^{16}O_2$ are located, is shown in the upper trace of Fig. 1. The traces in the middle part of Fig. 1 show a small part of the high resolution spectrum in the region of the Q- and R-branches of the $2\nu_3$ band. One can see a clearly pronounced detail structure of the spectrum. Because the $\nu_1+3\nu_2$ band is located very closely to the $2\nu_3$ band, one can expect.

(1) the presence of strong Fermi-type resonance interaction between these two bands, and
(2) probably, an appearance of transitions belonging to the $\nu_1+3\nu_2$ band caused by borrowing of intensity from the strong $2\nu_3$ band.

The assignment of the transitions of the $2\nu_3$ band was made on the basis of the ground state combination differences method. Here, the ground state rotational energies have been calculated with the parameters from Ref. [21] (for the convenience of the reader they are reproduced from [21] in column 2 of Table 3). About 2500 transitions with $J^{max.}=76$ and $K_a^{max.}=26$ were assigned to the $2\nu_3$ band (complete list of the assigned transitions together with the corresponding transmittances is presented electronically as Supplementary Material I of this paper; see also statistical information in Table 1). On that basis, we obtained 830 upper ro-vibrational energies of the (002) vibrational state from which a small part is presented as an illustration in Table 4 (column 2) together with experimental uncertainties (column 3).

The very weak $2\nu_1+\nu_2$ band also can be seen on the upper trace of Fig. 1 and in more details in Fig. 2. In spite of the weakness, its rotational structure is clearly pronounced, especially in the region of the P-branch. As for the $2\nu_3$ band, the assignment of transitions in the $2\nu_1+\nu_2$ band was made on the basis of the ground state combination differences method with known rotational energies of the ground vibrational state, and about 770 transitions with $J^{max.}=45$ and $K_a^{max.}=11$ were assigned to the $2\nu_1+\nu_2$ band for the first time. The list of the assigned transitions together with the corresponding transmittances is presented in the Supplementary Material II of this paper (see also statistical information in Table 1). The assigned transitions were used then for the determination of the ro-vibrational energies of the (210) vibrational states.

To improve the analysis of the rotational structure of the state (210), we additionally analyzed the spectrum in the region 2200–2380 cm^{-1} (see, Fig. 3, where both the survey spectrum, and the high resolution spectrum is shown), which was considered in the preceding study, Ref. [30]. Here the $2\nu_1+\nu_2-\nu_2$ hot band is located. While we were not able to assign transitions to the $2\nu_1+\nu_2-\nu_2$ band in the preceding study, in the present study, experimental information about the rotational structure of the (210) state, obtained from the analysis of the $2\nu_1+\nu_2$ band, gave us the possibility to assign, for the first time, more than 600 transitions with $J^{max.}=43$ and $K_a^{max.}=13$ to the $2\nu_1+\nu_2-\nu_2$ band (the rotational energies being necessary for the analysis of the lower (010) vibrational state have been calculated with the parameters from Ref. [21]). The list of the assigned transitions together with the corresponding transmittances is presented in the Supplementary Material III of this paper (see also statistical information in Table 1). Being added to the transitions assigned to the $2\nu_1+\nu_2$ band, these 600 transitions allowed us to obtain 302 energy values of the (120) vibrational state (as an illustration, part of the result is presented in column 2 of Table 5 together with their experimental uncertainties in column 3).

As discussed in Section 3, we used the effective Hamiltonian model, which takes into account resonance interactions between the states (002), (210), (130), and (050), for the theoretical analysis of the obtained experimental data. In this case, it is possible to make preliminary estimations of the values of parameters of the states (130) and (050), and the main resonance interaction parameters, as well as of the values of the high order centrifugal distortion parameters of the states (002) and (210). To make such

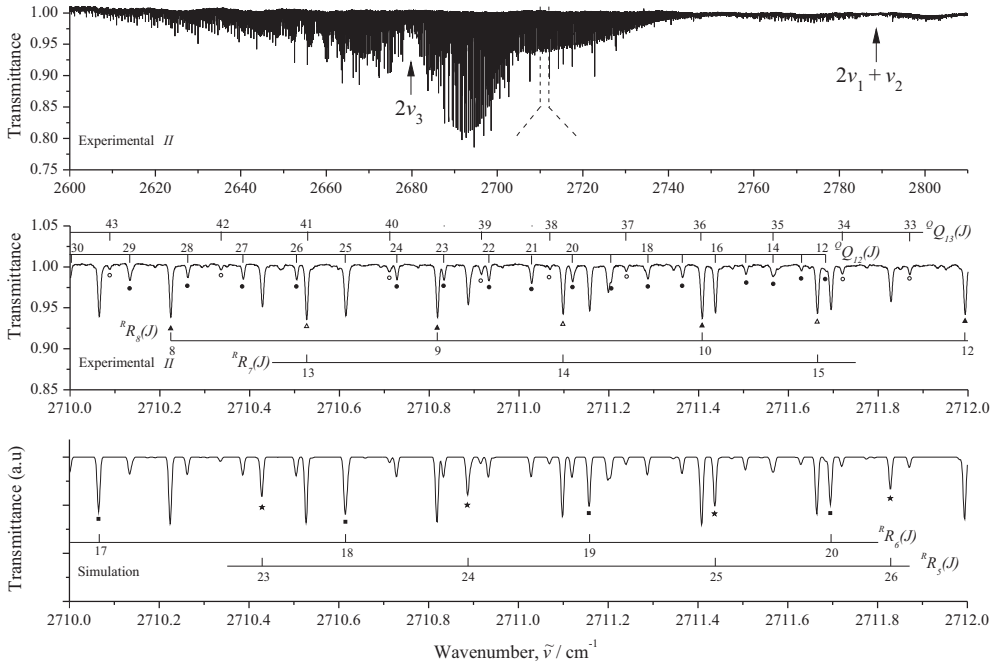

Fig. 1. Survey spectrum (upper trace) and a small part of the high resolution spectrum (middle trace) of $^{34}S^{16}O_2$ in the region of the $2\nu_3$ band. Experimental conditions: sample pressure is 480 Pa, absorption path length is 24 m; room temperature; number of scans is 1480. A few sets of transitions assigned to the $2\nu_3$ band are marked by circles, triangles, squares, and stars. The lower trace is the simulation spectrum (calculation was made with one, the main, dipole moment parameter and Doppler profile of the lines).

Table 3
Spectroscopic parameters of the (002), (210), (130), and (050) vibrational states of $^{34}S^{16}O_2$ (in cm^{-1}).[a]

Parameter	(000)[b]	(002)[c]	(002)[d]	(210)[c]	(210)[d]	(130)[c]	(130)[d]	(050)[c]
1	2	3	4	5	6	7	8	9
E		2679.800	2679.799765(11)	2789.02	2788.392891(68)	2676.01	2673.315(22)	2560.95
A	1.967733713	1.92879	1.92879114(22)	2.00703	2.0068847(16)	2.08816	2.08816	2.17624
B	0.3441883891	0.34188	0.341877009(64)	0.34099	0.34098805(40)	0.34273	0.34273	0.34443
C	0.2922455227	0.29008	0.290084867(46)	0.28897	0.28897928(27)	0.28928	0.289359(68)	0.28952
$\Delta_K \times 10^4$	0.81387956	0.7897	0.7897718(97)	0.9230	0.926386(98)	1.1104	1.1104	1.2633
$\Delta_{JK} \times 10^5$	−0.37222039	−0.4059	−0.404712(34)	−0.3607	−0.35636(23)	−0.4085	−0.4085	−0.4453
$\Delta_J \times 10^6$	0.21922689	0.2239	0.223959(45)	0.2187	0.21657(26)	0.2200	0.2200	0.2205
$\delta_K \times 10^6$	0.821985	0.6687	0.7005(21)	1.1890	1.108(14)	1.5009	1.5009	1.8903
$\delta_J \times 10^7$	0.5746703	0.5896	0.58812(19)	0.5737	0.5611(14)	0.5819	0.5819	0.5837
$H_K \times 10^7$	0.1122874	0.1062	0.106276(13)	0.1462	0.1462	0.2103	0.2103	0.2936
$H_{KJ} \times 10^9$	−0.596544	−0.4431	−0.46367(95)	−0.8391	−0.8391	−0.9446	−0.9446	−0.9178
$H_{JK} \times 10^{11}$	0.1645	0.1436	0.1436	0.6078	0.6078	0.7565	0.7565	1.5643
$H_J \times 10^{12}$	0.38599	0.3473	0.3963(91)	0.4603	0.4603	0.4220	0.4220	0.4206
$h_K \times 10^9$	0.55481	0.5548	0.5548	0.7099	0.7099	0.9000	0.9000	1.3342
$h_{JK} \times 10^{13}$	−0.381263781	−0.3813	−0.3813	−0.3813	−0.3813	−0.3813	−0.3813	−0.3813
$h_J \times 10^{12}$	0.185546	0.1855	0.1846(49)	0.1843	0.1843	0.1855	0.1855	0.1675
$L_K \times 10^{11}$	−0.209385	−0.205	−0.205	−0.307	−0.307	−0.487	−0.487	−0.583
$L_{KKJ} \times 10^{12}$	0.11361	0.114	0.114	0.139	0.139	0.180	0.180	0.138
$L_{JK} \times 10^{15}$	0.727503291	0.728	0.728	0.728	0.728	0.728	0.728	0.728
$L_{JJK} \times 10^{17}$	−0.687809164	−0.688	−0.688	−0.688	−0.688	−0.688	−0.688	−0.688
$L_J \times 10^{18}$	−0.324891428	−0.325	−0.325	−0.325	−0.325	−0.325	−0.325	−0.325
$P_K \times 10^{15}$	0.29672	0.30	0.30	0.48	0.48	0.82	0.82	1.07
$P_{KKKJ} \times 10^{16}$	−0.2314	−0.23	−0.23	−0.23	−0.23	−0.23	−0.23	−0.23
$P_{KKJ} \times 10^{17}$	0.13312543	0.13	0.13	0.13	0.13	0.13	0.13	0.13

[a] Values in parentheses are 1σ statistical confidence intervals (in last digits). Parameters presented without confidence intervals have been constrained to values estimated theoretically (see text for details).
[b] Reproduced from Ref. [21].
[c] Predicted theoretically (see text for details).
[d] Obtained from the fit of experimental ro-vibrational energy values.

estimations, we used the same argument as in the preceding paper, Ref. [30], namely:

(1) The unperturbed vibrational energies of the states (210), (130) and (050) and the main Fermi interaction parameters, have been estimated on the basis of the results and formulas of the isotopic substitution theory, Refs. [34–36].
(2) Initial values of the A, B and C rotational parameters of all four vibrational states, (002), (210), (130) and (050), were estimated on the basis of known values of the equilibrium rotational parameters A_e, B_e and C_e, as well as the α and γ vibration–rotation coefficients from Table 4 of Ref. [22].
(3) To estimate the values of the centrifugal distortion coefficient of the states (002), (210) and (130), we used the following simple relations, which showed very good predictive power in study of analogous XY_2 (C_{2v}) molecules (see Refs. [45–47]):

$$P^{(v_1 v_2 v_3)} = P^{(0 v_2 0)} + v_1 (P^{(100)} - P^{(000)}) + v_3 \left(P^{(001)} - P^{(000)} \right), \quad (4)$$

where P denotes any of the centrifugal distortion parameters; the values of the initial parameters of the (000), (100), (001), (010), (020), and (030) vibrational states were taken from Refs. [21,22].
(4) To estimate the values of parameters of the (050) state (with the exception of the parameter H_K), we used another simple relation which also showed a good prediction power for estimation of parameters of highly excited vibrational states in the XY_2 (C_{2v}) type molecules (see, e.g., Ref. [48]):

$$P^{(0 v_2 0)} = P^{(000)} + v_2 \Delta p_1 + v_2^2 \Delta p_2 + v_2^3 \Delta p_3, \quad (5)$$

where $P^{(000)}$ is the value of a centrifugal distortion coefficient of the ground vibrational state; the coefficients Δp_1, Δp_2, and Δp_3 can be determined from the values of corresponding centrifugal distortion coefficient of the states (010), (020), and (030). The following remark should be made here: as the visible inspection of the H_K-values for the set of the states (000), (010), (020) and (030) shows (see Refs. [21,22]), there is a missprint in the value of the H_K parameters of the state (030) in Table 2 of Ref. [22]. On that reason, to estimate the H_K-value for the (050) vibrational state we used a more rough approximation in formula (5), namely, $\Delta p_3 = 0$ for the H_K parameters.

Results of the above discussed estimations are shown in columns 3, 5, 7 and 9 of Table 3. They were used then as the initial approximation in the weighted fit procedure with the effective Hamiltonian, Eqs. (1)–(3). As the result of the fit, we obtained a set of 30 fitted parameters, which are presented in columns 4, 6 and 8 of Table 3 and in Table 6. The values of 1σ statistical confidence intervals for fitted parameters (in last digits) are also shown in parentheses. Parameters presented without confidence intervals have been constrained to values estimated theoretically (see above). Strong local resonance interactions between the states $[JK_aK_c]$ of (002) and the same, $[JK_aK_c]$ states of (130) for the values of $K_a = 5$, 6, and 7 allowed us to fit the parameters E and C of the (130) vibrational state, as well.

The parameters obtained from the fit reproduce the 830 initial energy values of the (002) vibrational state (about 2500 transition assigned to the $2v_3$ band) with the $d_{rms} = 1.2 \times 10^{-4}$ cm^{-1}. For illustration of the quality of the fit, column 4 of Table 4 presents differences δ between experimental and calculated values of the individual ro-vibrational energy values. One can see rather good

Table 4
Small part of experimental ro-vibrational term values for the (002) vibrational state of $^{34}S^{16}O_2$ (in cm^{-1}).[a]

J	K_a	K_c	E	Δ	δ	J	K_a	K_c	E	Δ	δ	J	K_a	K_c	E	Δ	δ	J	K_a	K_c	E	Δ	δ
1			2	3	4	1			2	3	4	1			2	3	4	1			2	3	4
10	0	10	2713.9832	0	0	14	7	7	2825.0880	1	0	17	17	1	3236.5679	1	2	20	16	4	3220.8080	0	1
10	1	9	2717.4296	1	1	14	8	6	2849.1469	2	0	18	0	18	2783.8719	1	0	20	17	3	3272.7270		0
10	2	8	2721.4899	1	0	14	9	5	2876.3766	1	0	18	1	17	2791.9502	0	0	20	18	2	3327.6247		−1
10	3	7	2729.1727	1	0	14	10	4	2906.7607	1	0	18	2	16	2797.2636	2	1	20	19	1	3385.4741	2	1
10	4	6	2740.3981	1	0	14	11	3	2940.2811	1	−1	18	3	15	2803.5943	2	0	20	20	0	3446.2461		0
10	5	5	2754.8709	1	0	14	12	2	2976.9193	1	0	18	4	14	2814.1238	1	0	21	1	21	2819.6234		0
10	6	4	2772.5545	1	0	14	13	1	3016.6545	2	0	18	5	13	2828.4312	1	1	21	2	20	2830.5177	1	0
10	7	3	2793.4325	1	1	14	14	0	3059.4655	2	1	18	6	12	2846.0516	1	−1	21	3	19	2840.7351	0	0
10	8	2	2817.4935	3	0	15	1	15	2753.5635	0	0	18	7	11	2866.8995	1	0	21	4	18	2852.2368	2	1
10	9	1	2844.7222	1	1	15	2	14	2761.6225	1	0	18	8	10	2890.9475	2	0	21	5	17	2866.5541	1	1
10	10	0	2875.1028	2	2	15	3	13	2770.3835	1	0	18	9	9	2918.1736	2	1	21	6	16	2884.1205	0	1
11	1	11	2721.2245	1	−1	15	4	12	2781.6368	1	0	18	10	8	2948.5583	1	−1	21	7	15	2904.9357	1	0
11	2	10	2727.8273	0	0	15	5	11	2796.0630	2	0	18	11	7	2982.0832	1	0	21	8	14	2928.9660	1	0
11	3	9	2736.1179	1	0	15	6	10	2813.7215	1	−1	18	12	6	3018.7282	1	0	21	9	13	2956.1832	1	0
11	4	8	2747.3696	0	1	15	7	9	2834.5880	1	0	18	13	5	3058.4725	1	1	21	10	12	2986.5651	1	−1
11	5	7	2761.8373	1	0	15	8	8	2858.6451	1	−1	18	14	4	3101.2942	0	1	21	11	11	3020.0912	1	0
11	6	6	2779.5182	2	0	15	9	7	2885.8746	1	0	18	15	3	3147.1702	2	1	21	12	10	3056.7402	1	−1
11	7	5	2800.3953	1	1	15	10	6	2916.2592	2	0	18	16	2	3196.0761	1	1	21	13	9	3096.4912	2	1
11	8	4	2824.4561	2	−1	15	11	5	2949.7810	1	0	18	17	1	3247.9867	1	1	21	14	8	3139.3214	2	1
11	9	3	2851.6854	2	0	15	12	4	2986.4209	1	0	18	18	0	3302.8753		1	21	15	7	3185.2073	2	−1
11	10	2	2882.0668	2	−1	15	13	3	3026.1584	2	0	19	1	19	2795.2734	0	0	21	16	6	3234.1252	2	2
11	11	1	2915.5832	1	−1	15	14	2	3068.9719	0	1	19	2	18	2805.1533	1	0	21	17	5	3286.0484	2	−1
12	0	12	2728.0011	1	−1	16	0	16	2762.9485	0	0	19	3	17	2814.7763	1	1	21	18	4	3340.9511	2	−1
12	1	11	2732.3721	1	0	16	1	15	2769.6907	0	0	19	4	16	2826.1402	2	0	21	19	3	3398.8059		2
12	2	10	2736.4376	1	1	16	2	14	2774.3520	0	−1	19	5	15	2840.4957	2	−1	21	20	2	3459.5834		0
12	3	9	2743.8218	1	0	16	3	13	2780.9942	1	1	19	6	14	2858.1029	1	1	21	21	1	3523.2547		−1
12	4	8	2754.9819	1	1	16	4	12	2791.8303	1	1	19	7	13	2878.9418	2	2	22	0	22	2832.6371	1	−1
12	5	7	2769.4391	2	−1	16	5	11	2806.2135	1	0	19	8	12	2902.9849	2	1	22	1	21	2843.4157	1	0
12	6	6	2787.1164	1	0	16	6	10	2823.8616	2	1	19	9	11	2930.2086	1	0	22	2	20	2850.7607	1	1
12	7	5	2807.9919	1	0	16	7	9	2844.7230	1	0	19	10	10	2960.5931	1	1	22	3	19	2856.9528	2	−1
12	8	4	2832.0526	1	0	16	8	8	2868.7780	1	1	19	11	9	2994.1184	1	0	22	4	18	2866.5671	2	1
12	9	3	2859.2821	1	−1	16	9	7	2896.0067	1	0	19	12	8	3030.7649	0	0	22	5	17	2880.5672	3	2
12	10	2	2889.6646	1	0	16	10	6	2926.3916	1	0	19	13	7	3070.5114	3	0	22	6	16	2898.0889	1	1
12	11	1	2923.1825	2	1	16	11	5	2959.9146	2	0	19	14	6	3113.3360	2	1	22	7	15	2918.8884	1	0
12	12	0	2959.8170	0	0	16	12	4	2996.5563	1	1	19	15	5	3159.2154	2	2	22	8	14	2942.9105	2	1
13	1	13	2736.2177	1	0	16	13	3	3036.2961	2	2	19	16	4	3208.1248	2	−1	22	9	13	2970.1231	1	0
13	2	12	2743.4976	1	1	16	14	2	3079.1121	1	0	19	17	3	3260.0395	3	−1	22	10	12	3000.5030	2	−1
13	3	11	2751.9801	1	1	16	15	1	3124.9818	1	2	19	18	2	3314.9328		0	22	11	11	3034.0290	2	1
13	4	10	2763.2260	1	0	16	16	0	3173.8804	1	0	19	19	1	3372.7770		1	22	12	10	3070.6790	1	0
13	5	9	2777.6771	2	1	17	1	17	2773.2514	1	0	20	0	20	2807.1000	0	0	22	13	9	3110.4319	2	0
13	6	8	2795.3494	3	−1	17	2	16	2782.1815	1	0	20	1	19	2816.5369	1	0	22	14	8	3153.2651	1	2
13	7	7	2816.2228	0	1	17	3	15	2791.3199	1	0	20	2	18	2822.7519	3	0	22	15	7	3199.1545	2	0
13	8	6	2840.2827	0	0	17	4	14	2802.6070	3	0	20	3	17	2828.9117	1	1	22	16	6	3248.0760	2	−1
13	9	5	2867.5125	1	0	17	5	13	2817.0007	1	0	20	4	16	2839.0260	1	1	22	17	5	3300.0040	2	−1
13	10	4	2897.8958	3	0	17	6	12	2834.6380	1	0	20	5	15	2853.2124	1	0	22	18	4	3354.9120		1
13	11	3	2931.4150	3	0	17	7	11	2855.4935	1	1	20	6	14	2870.7924	1	−1	22	19	3	3412.7722		3
13	12	2	2968.0514	1	1	17	8	10	2879.5454	3	1	20	7	13	2891.6203	2	1	22	21	1	3537.2329		−2
13	13	1	3007.7845	1	0	17	9	9	2906.7729	1	0	20	8	12	2915.6576	1	0	22	22	0	3603.7742		−6
14	0	14	2744.3255	0	0	17	10	8	2937.1579	2	−1	20	9	11	2942.8784	0	0	23	1	23	2846.2974	1	0
14	1	13	2749.8113	1	0	17	11	7	2970.6819	1	−1	20	10	10	2973.2620	2	1	23	2	22	2858.2561	1	0
14	2	12	2754.0648	0	0	17	12	6	3007.3253	1	0	20	11	9	3006.7880	2	3	23	3	21	2869.1761	0	0
14	3	11	2761.0830	1	1	17	13	5	3047.0674	2	1	20	12	8	3043.4357	2	1	23	4	20	2880.8935	1	0
14	4	10	2772.1217	1	−1	17	14	4	3089.8861	1	−1	20	13	7	3083.1844	2	1	23	5	19	2895.1810	2	−1
14	5	9	2786.5515	3	−1	17	15	3	3135.7589	1	0	20	14	6	3126.0118	3	1	23	6	18	2912.6959	2	2
14	6	8	2804.2178	2	1	17	16	2	3184.6610	3	−2	20	15	5	3171.8944	1	1	23	7	17	2933.4789	1	0

[a] In Table 4, Δ is the experimental uncertainty of the energy value, equal to one standard error in units of 10^{-4} cm^{-1}; δ is the difference $E^{exp.} - E^{calc.}$, also in units of 10^{-4} cm^{-1}. When the Δ-value is absent, the corresponding energy level was determined from the single transition and was used in the fit with the weight of 1/100.

correlation between experimental and calculated values (see also statistical information in Table 1). As to the (210) vibrational state, one can see in column 4 of Table 5, that the experimental values of ro-vibrational energies are reproduced with a worse accuracy. The reason is in the fact, that both the $2v_1 + v_2$ cold band, and the $2v_1 + v_2 - v_2$ hot band are very weak. As the consequence, accuracy in transitions of both bands are considerably worse in comparison with the accuracy in line positions in the strong $2v_3$ band. As the resume, the $d_{rms} = 3.7 \times 10^{-4}$ cm^{-1} was produced for the 302 ro-vibrational energy levels of the (210) vibrational state (for more details, see, Table 1). As one more confirmation of the correctness of the results of the fit, on the one hand, and the correctness of the values of ro-vibrational coefficients from Ref. [22] and Eqs. (4) and (5) of the present paper, on the other hand, one can compare the theoretically predicted with the spectroscopically obtained (from the fit) values of spectroscopic parameters. It is seen that all of them rather good correlate with each other.

5. Conclusion

In the present study, we reanalyzed the high resolution rotational structure of the $2v_3$ band of the $^{34}S^{16}O_2$ molecule. The spectrum was recorded with a Bruker IFS 120 HR Fourier transform

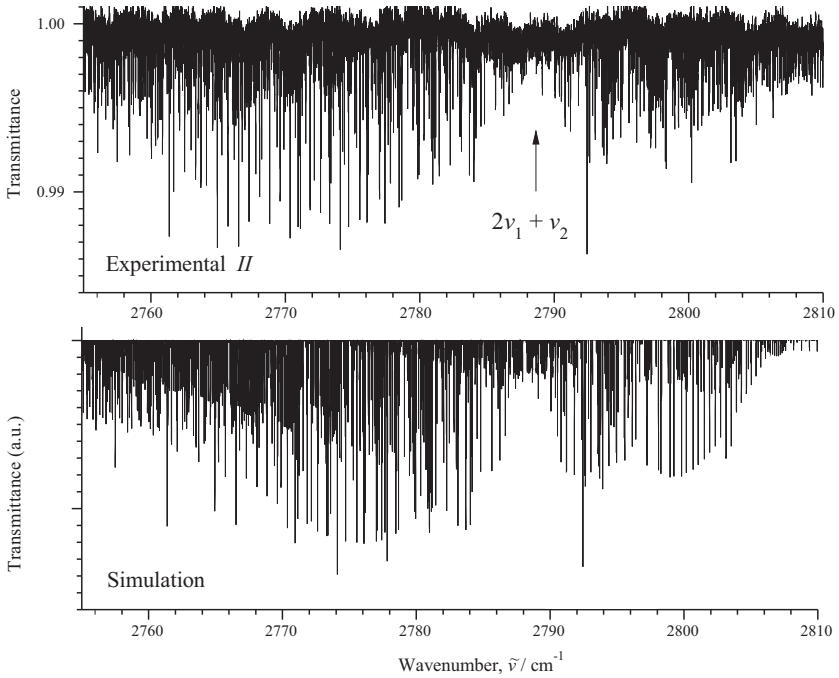

Fig. 2. More detailed survey spectrum (upper trace) of $^{34}S^{16}O_2$ in the region of the $2\nu_1 + \nu_2$ band (for the experimental conditions, see caption to Fig. 1). The lower trace is the simulation spectrum (calculation was made with one, the main, dipole moment parameter and Doppler profile of the lines).

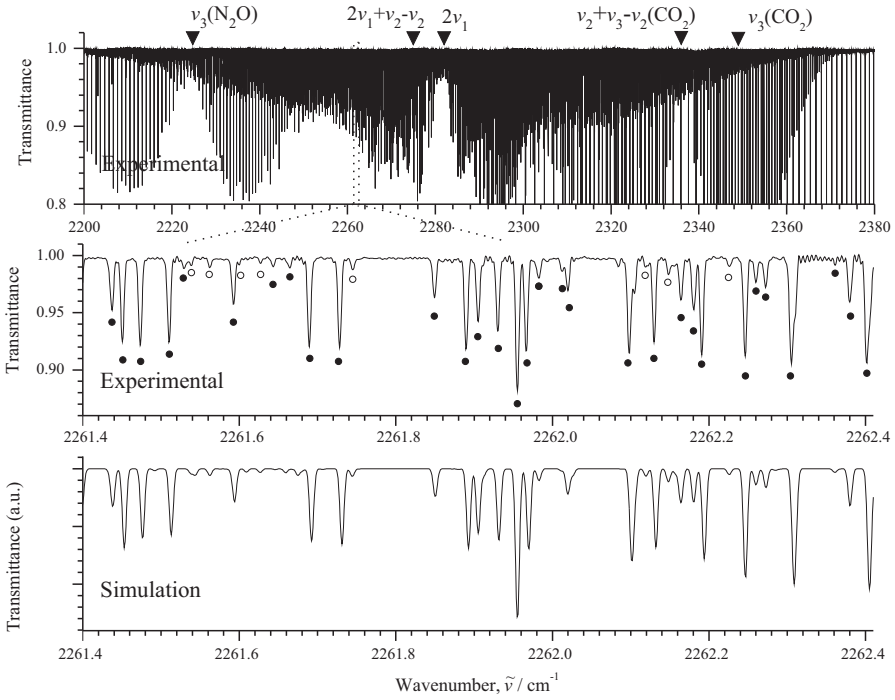

Fig. 3. Survey spectrum (upper trace, reproduced from the preceding Ref. [30]) and a small part of the high resolution spectrum (middle trace) of $^{34}S^{16}O_2$ in the region of the hot $2\nu_1 + \nu_2 - \nu_2$ band. Experimental conditions: sample pressure is 10 Pa, absorption path length is 8 m; room temperature; number of scans is 550. Centers of the $2\nu_1 + \nu_2 - \nu_2$ and $2\nu_1$ bands of $^{34}S^{16}O_2$, as well as of the ν_3 and $\nu_2 + \nu_3 - \nu_2$ bands of CO_2 and ν_3 band of N_2O are marked in the upper trace. Lines assigned to the $2\nu_1 + \nu_2 - \nu_2$ and $2\nu_1$ bands of $^{34}S^{16}O_2$ are marked by open and dark circles, respectively, in the middle trace. The lower trace is the simulation spectrum (calculations of relative line strengths both for the $2\nu_1$ band, and for the $2\nu_1 + \nu_2 - \nu_2$ band were made with only one, the main, dipole moment parameter and Doppler profile of the lines).

interferometer in the infrared laboratory of the Technische Universität Braunschweig (Germany). About 2500 transitions with maximum values of quantum numbers $J^{max.} = 76$ and $K_a^{max.} = 26$ were assigned to the $2\nu_3$ band. The very weak $2\nu_1 + \nu_2$ band was also recorded and analyzed for the first time. It gave us the possibility to find, also for the first time, the hot band $2\nu_1 + \nu_2 - \nu_2$, which is located in the 2200–2380 cm^{-1} region and totally covered by the considerably stronger $2\nu_1$ band. In general, about 1370 transitions with maximum values of quantum numbers $J^{max.} = 45$ and $K_a^{max.} = 13$ were assigned to the bands $2\nu_1 + \nu_2$ and $2\nu_1 + \nu_2 - \nu_2$,

Table 5
Small part of experimental ro-vibrational term values for the (210) vibrational state of $^{34}S^{16}O_2$ (in cm^{-1}).[a]

J	K_a	K_c	E	Δ	δ	J	K_a	K_c	E	Δ	δ	J	K_a	K_c	E	Δ	δ	J	K_a	K_c	E	Δ	δ
1			2	3	4	1			2	3	4	1			2	3	4	1			2	3	4
10	0	10	2822.7312	4	−4	15	1	15	2862.2466	2	−1	19	5	15	2950.9134	5	2	23	10	14	3131.1264	4	0
10	1	9	2826.2512	4	−1	15	2	14	2870.5565	4	−1	19	6	14	2969.3845	4	3	23	11	13	3166.2502	4	−4
10	3	7	2838.6096	3	2	15	3	13	2879.6914	4	0	19	7	13	2991.2394	2	1	24	0	24	2968.8260	4	2
10	4	6	2850.3892	3	−4	15	4	12	2891.4930	5	3	19	8	12	3016.4475	2	1	24	1	23	2981.1436	5	2
10	6	4	2884.1166	2	−1	15	5	11	2906.6282	3	0	19	9	11	3044.9838	4	1	24	2	22	2989.8441	4	−2
10	7	3	2906.0108	3	0	15	6	10	2925.1496	3	2	19	10	10	3076.8256	5	−4	24	3	21	2996.5306		1
10	8	2	2931.2375	5	−1	15	7	9	2947.0317	4	−1	19	11	9	3111.9521	3	0	24	5	19	3020.6822	4	0
10	9	1	2959.7803	6	−3	15	8	8	2972.2540	3	−1	19	12	8	3150.3391		1	24	6	18	3038.9936	5	1
11	1	11	2830.0104	5	−1	15	9	7	3000.7967	5	−1	19	13	7	3191.9623	2	−4	24	7	17	3060.7731	5	−2
11	2	10	2836.8565	4	−2	15	10	6	3032.6403	4	−2	20	0	20	2915.6031	4	0	24	8	16	3085.9394	4	2
11	3	9	2845.5349	4	4	15	11	5	3067.7646	4	4	20	1	19	2925.1874	2	1	24	9	15	3114.4521	6	−1
11	4	8	2857.3388	4	5	15	12	4	3106.1458		−4	20	2	18	2931.4765	4	0	24	10	14	3146.2830	2	0
11	5	7	2872.5150	5	3	15	13	3	3147.7623		−5	20	3	17	2937.9609	4	−4	24	12	12	3219.7950	3	−3
11	6	6	2891.0577	3	−2	16	0	16	2871.5770	3	−1	20	4	16	2948.6746	5	−1	25	1	25	2983.5880	2	−2
11	7	5	2912.9509	2	0	16	1	15	2878.4070	3	2	20	5	15	2963.5862	4	3	25	2	24	2996.9656	2	1
11	8	4	2938.1776	2	1	16	2	14	2883.2030	4	1	20	6	14	2982.0315	4	−1	25	3	23	3009.0209	4	0
11	9	3	2966.7209	4	2	16	3	13	2890.2379	4	1	20	7	13	3003.8759	1	0	25	4	22	3021.5352	4	−1
11	11	1	3033.6818	4	0	16	4	12	2901.6491	5	1	20	8	12	3029.0778	5	−3	25	5	21	3036.5096	3	3
12	0	12	2836.7171	2	0	16	5	11	2916.7446	2	−4	20	9	11	3057.6117	4	2	25	6	20	3054.8279	2	2
12	1	11	2841.1590	4	−2	16	6	10	2935.2559	3	−2	20	10	10	3089.4527	3	2	25	7	19	3076.5877	4	2
12	2	10	2845.4132	4	−3	16	7	9	2957.1335	3	0	20	11	9	3124.5785	1	−1	25	8	18	3101.7404	3	−2
12	3	9	2853.2072	3	2	16	8	8	2982.3533	4	−1	20	12	8	3162.9666	3	1	25	9	17	3130.2463	2	4
12	4	8	2864.9257	6	4	16	9	7	3010.8953	5	0	21	1	21	2928.0978	1	−2	25	11	15	3197.1931	2	−2
12	5	7	2880.0921	2	3	16	10	6	3042.7385	4	−5	21	2	20	2939.2730	5	0	26	0	26	2998.8928	1	1
12	6	6	2898.6310	5	−3	16	11	5	3077.8634	3	−2	21	3	19	2949.8357	2	−1	26	1	25	3012.5233	2	2
12	7	5	2920.5223	4	−5	16	12	4	3116.2467	2	−1	21	4	18	2961.8599	2	3	26	2	24	3022.6570	2	−3
12	8	4	2945.7490	5	1	17	1	17	2881.8725	1	−1	21	5	17	2976.8843	5	4	26	5	21	3053.1087	4	2
12	9	3	2974.2926	4	3	17	2	16	2891.0604	5	0	21	6	16	2995.3152	3	1	26	6	20	3071.3083	3	−1
12	10	2	3006.1342	3	−3	17	3	15	2900.5637	3	1	21	7	15	3017.1468	5	−4	26	7	19	3093.0380	6	−9
12	11	1	3041.2551	2	−1	17	4	14	2912.3933	3	−1	21	8	14	3042.3427	3	3	26	8	18	3118.1766	4	−4
12	12	0	3079.6327		−2	17	5	13	2927.4967	4	1	21	9	13	3070.8724	3	4	26	9	17	3146.6735	2	0
13	1	13	2844.9557	3	−1	17	6	12	2945.9970	2	−1	21	10	12	3102.7114	2	1	27	1	27	3014.8000	2	−3
13	2	12	2852.4819	3	−1	17	7	11	2967.8685	4	0	21	11	11	3137.8373	5	1	27	2	26	3029.3277	2	1
13	3	11	2861.3457	4	−2	17	8	10	2993.0851	4	−2	21	13	9	3217.8528	5	1	27	3	25	3042.2750	3	−2
13	4	10	2873.1430	4	3	17	9	9	3021.6256	6	−2	22	0	22	2941.0632	1	−2	27	4	24	3055.1823	5	1
13	5	9	2888.3026	5	0	17	10	8	3053.4696	3	2	22	1	21	2952.0307	2	3	27	5	23	3070.1727	5	0
13	6	8	2906.8376	4	1	17	11	7	3088.5948	5	1	22	2	20	2959.4288	4	2	27	6	22	3088.4199	3	−1
13	7	7	2928.7267	2	0	17	12	6	3126.9790		−3	22	3	19	2965.8935	3	1	27	7	21	3110.1279	3	5
13	8	6	2953.9517	4	−3	18	0	18	2892.4428	3	0	22	4	18	2976.1087	4	−6	27	8	20	3135.2487	1	−1
13	9	5	2982.4955	4	0	18	1	17	2900.6335	4	3	22	5	17	2990.8463	5	−2	27	9	19	3163.7349	4	−3
13	10	4	3014.3387	6	4	18	2	16	2906.0500	5	0	22	6	16	3009.2370	4	4	27	11	17	3230.6658	6	−4
13	11	3	3049.4603	4	2	18	3	15	2912.7463	2	−3	22	7	15	3031.0536	3	0	28	0	28	3031.2652	4	0
13	12	2	3087.8390	3	−2	18	4	14	2923.8642	4	1	22	8	14	3056.2408	4	3	28	2	26	3057.8040	3	−1
14	0	14	2853.0019	2	−1	18	5	13	2938.8889	5	4	22	9	13	3084.7654	4	0	28	3	25	3065.7668	3	−3
14	1	13	2858.5623	3	−1	18	6	12	2957.3731	5	1	22	10	12	3116.6024	5	−2	28	6	22	3106.1891	3	2
14	2	12	2862.9792	4	−5	18	7	11	2979.2369	2	−1	22	11	11	3151.7278	2	0	28	7	21	3127.8549	4	3
14	3	11	2870.4043	5	1	18	8	10	3004.4496	5	−2	23	1	23	2954.6867	0	0	28	8	20	3152.9569	4	4
14	4	10	2882.0083	3	3	18	9	9	3032.9890	4	4	23	2	22	2966.9429	2	2	28	9	19	3181.4317	4	4
14	5	9	2897.1489	4	8	18	10	8	3064.8317	3	0	23	3	21	2978.2004	2	4	29	1	29	3048.3214	2	−2
14	6	8	2915.6765	3	−2	18	11	7	3099.9576	1	1	23	4	20	2990.4240		0	29	2	28	3064.0184	5	0
14	7	7	2937.5631	3	1	18	12	6	3138.3431	2	−2	23	5	19	3005.4140	3	−2	29	3	27	3077.9398	4	3
14	8	6	2962.7872	3	2	19	1	19	2903.8249	3	−3	23	6	18	3023.7951	4	5	29	4	26	3091.3494	3	2
14	9	5	2991.3300	4	−3	19	2	18	2913.9726	1	0	23	7	17	3045.5957	4	3	29	5	25	3106.4057	3	2
14	10	4	3023.1734	5	−2	19	3	17	2923.9504	5	0	23	8	16	3070.7730	4	3	29	6	24	3124.5769	3	0
14	11	3	3058.2962	2	−2	19	4	16	2935.8489	3	3	23	9	15	3099.2925	4	4	29	8	22	3171.3004		1

[a] See footnote to Table 4.

Table 6
Resonance interaction parameters for some sets of vibrational states of $^{34}S^{16}O_2$ (in cm^{-1}).[a]

Parameter	Value	Parameter	Value	Parameter	Value
$^{(002),(210)}F_{xy} \times 10^4$	0.625(88)				
$^{(002),(130)}F_K \times 10^3$	0.4851(21)	$^{(002),(130)}F_{xy} \times 10^4$	0.209(26)	$^{(002),(130)}F_{Kxy} \times 10^6$	−0.307(35)
$^{(002),(130)}F_{Jxy} \times 10^8$	−0.381(97)	$^{(002),(130)}F_{KKxy} \times 10^8$	0.324(14)		
$^{(210),(130)}F_0$	5.32				
$^{(130),(050)}F_0$	6.86				

[a] Values in parentheses are 1σ statistical confidence intervals (in last digits). Parameters presented without confidence intervals have been constrained to values estimated theoretically (see text for details).

and 302 ro-vibrational energies of the (210) state were determined. Being used in the weighted fit, the 1132 experimental ro-vibrational energies of the (002) and (210) vibrational states allowed us to obtain a set of 30 spectroscopic parameters which reproduces the initial "experimental" energy values with the $d_{rms} = 1.2 \times 10^{-4}$ cm^{-1} and 3.7×10^{-4} cm^{-1} for the states (002) and (210), respectively.

Acknowledgments

The work was supported by the project "Leading Russian Research Universities" (Grant FTI-120 of the Tomsk Polytechnic University). Part of the work was supported by the Foundation of the President of the Russian Federation (Grant MK-4872.2014.2), by the Deutsche Forschungsdemeinschaft (Grants BA 2176/3-2, BA 2176/4-1, BA 2176/4-2, and BA 2176/5-1) and by the DAAD Grants Nos. 91578560, 91578563 and 91578568.

Appendix A. Supplementary material

Supplementary data for this article are available on ScienceDirect (http://www.sciencedirect.com) and as part of the Ohio State University Molecular Spectroscopy Archives (http://library.osu.edu/sites/msa/jmsa_hp.htm).

Supplementary data associated with this article can be found, in the online version, at http://dx.doi.org/10.1016/j.jms.2015.09.009.

References

[1] O.N. Ulenikov, E.S. Bekhtereva, V.-M. Horneman, S. Alanko, O.V. Gromova, J. Mol. Spectrosc. 255 (2009) 111.
[2] O.N. Ulenikov, E.S. Bekhtereva, V.-M. Horneman, S. Alanko, O.V. Gromova, C. Leroy, J. Mol. Spectrosc. 257 (2009) 137.
[3] O.N. Ulenikov, E.S. Bekhtereva, O.V. Gromova, S. Alanko, V.-M. Horneman, C. Leroy, Molec. Phys. 108 (2010) 1253.
[4] O.N. Ulenikov, O.V. Gromova, E.S. Bekhtereva, I.B. Bolotova, C. Leroy, V.-M. Horneman, S. Alanko, J. Quant. Spectrosc. Radiat. Transfer 112 (2011) 486.
[5] O.N. Ulenikov, O.V. Gromova, E.S. Bekhtereva, I.B. Bolotova, I.A. Konov, V.-M. Horneman, C. Leroy, J. Quant. Spectrosc. Radiat. Transfer 113 (2012) 500.
[6] O.N. Ulenikov, O.V. Gromova, E.S. Bekhtereva, A.S. Belova, S. Bauerecker, C. Maul, C. Sydow, V.-M. Horneman, J. Quant. Spectrosc. Radiat. Transfer 144 (2014) 1.
[7] L.E. Snyder, J.M. Hollis, B.L. Ulich, F.J. Lovas, D.R. Johnson, D. Buhl, Astrophys. J. 198 (1975) 81.
[8] L.W. Esposito, J.R. Winick, A.I. Stewart, Geophys. Res. Lett. 6 (1979) 601.
[9] S. Self, M.R. Rampino, J.J. Barbera, J. Volcanol. Geotherm. Res. 11 (1981) 41.
[10] R.J. Charlson, T.L. Anderson, R.E. McDuff, in: S.S. Butcher, R.J. Charlson, G.H. Orian, G.V. Wolfe (Eds.), Global biogeochemical cycles, Academic, London, 1992, p. 285.
[11] B. Bézard, C. DeBergh, B. Fegley, J.-P. Maillard, D. Crips, T. Owen, J.B. Pollack, D. Grinspoon, Geophys. Res. Lett. 20 (1993) 1587.
[12] M.P. McCormic, L.W. Thompson, C.R. Trepte, Nature 373 (1995) 399.
[13] R.W. Carlson, W.D. Smythe, R.M.C. Lopes-Gautier, A.G. Davies, L.W. Kamp, J.A. Mosher, L.A. Soderblom, F.E. Leader, R. Mehlman, R.N. Clark, F.P. Fanale, Geophys. Res. Lett. 24 (1997) 2479.
[14] P.J. Wallace, J. Volcanol. Geotherm. Res. 108 (2001) 85.
[15] E. Marcq, J.-L. Betraux, F. Montmessin, D. Belyaev, Nature Geosci. 6 (2013) 25.
[16] O.N. Ulenikov, G.A. Onopenko, O.V. Gromova, E.S. Bekhtereva, V.-M. Horneman, J. Quant. Spectrosc. Radiat. Transfer 130 (2013) 220.
[17] Y. Morino, Y. Kukuchi, S. Saito, E. Hirota, J. Mol. Spectrosc. 13 (1964) 95.
[18] R. Van Riet, Ann. Soc. Sci. Bruxelles 78 (1964) 237.
[19] S.P. Belov, M.Y. Tretyakov, I.N. Kozin, E. Klisch, G. Winnewisser, W.J. Lafferty, J.-M. Flaud, J. Mol. Spectrosc. 191 (1998) 17.
[20] J. Henningsen, A. Barbe, M.-R. De Backer-Barilly, J. Quant. Spectrosc. Radiat. Transfer 109 (2008) 2491.
[21] W.J. Lafferty, J.-M. Flaud, R.L. Sams, El.H.A. Ngom, J. Mol. Spectrosc. 252 (2008) 72.
[22] W.J. Lafferty, J.-M. Flaud, El.H.A. Ngom, R.L. Sams, J. Mol. Spectrosc. 253 (2009) 51.
[23] J.-M. Flaud, W.J. Lafferty, R.L. Sams, J. Quant. Spectrosc. Radiat. Transfer 110 (2009) 669.
[24] A. Barbe, C. Secroun, P. Jouve, B. Duterage, N. Monnanteuil, J. Bellet, Mol. Phys. 34 (1977) 127.
[25] A.S. Pine, G. Dresselhaus, B. Palm, R.W. Davies, S.A. Clough, J. Mol. Spectrosc. 67 (1977) 386.
[26] G. Guelachvili, O.V. Naumenko, O.N. Ulenikov, J. Mol. Spectrosc. 125 (1987) 128.
[27] G. Guelachvili, O.V. Naumenko, O.N. Ulenikov, J. Mol. Spectrosc. 131 (1988) 400.
[28] O.N. Ulenikov, E.S. Bekhtereva, Yu.V. Krivchikova, Yu.B. Morzhikova, T. Buttersack, C. Sydow, S. Bauerecker, J. Quant. Spectrosc. Radiat. Transfer 166 (2015) 13.
[29] O.N. Ulenikov, E.S. Bekhtereva, Yu.V. Krivchikova, V.A. Zamotaeva, T. Buttersack, C. Sydow, S. Bauerecker, J. Quant. Spectrosc. Radiat. Transfer 168 (2016) 29.
[30] O.N. Ulenikov, E.S. Bekhtereva, O.V. Gromova, T. Buttersack, C. Sydow, S. Bauerecker, J. Quant. Spectrosc. Radiat. Transfer, accepted for publication.
[31] J.-M. Flaud, C. Camy-Peyret, J. Mol. Spectrosc. 55 (1975) 278.
[32] O.N. Ulenikov, G.A. Ushakova, J. Mol. Spectrosc. 117 (1986) 195.
[33] X.-H. Wang, O.N. Ulenikov, G.A. Onopenko, E.S. Bekhtereva, S.-G. He, S.-M. Hu, H. Lin, Q.-S. Zhu, J. Mol. Spectrosc. 200 (2000) 25.
[34] A.D. Bykov, Yu.S. Makushkin, O.N. Ulenikov, J. Mol. Spectrosc. 85 (1981) 462.
[35] A.D. Bykov, Yu.S. Makushkin, O.N. Ulenikov, J. Mol. Spectrosc. 93 (1982) 46.
[36] O.N. Ulenikov, E.S. Bekhtereva, G.A. Onopenko, E.A. Sinitsin, H. Bürger, W. Jerzembeck, J. Mol. Spectrosc. 208 (2001) 236.
[37] D. Papousek, M.R. Aliev, Elsevier, Amsterdam, 1982.
[38] Yu.S. Makushkin, O.N. Ulenikov, J. Mol. Spectrosc. 68 (1977) 1.
[39] O.N. Ulenikov, R.N. Tolchenov, Q.-S. Zhu, Spectrochim. Acta A 52 (1996) 1829.
[40] J.K.G. Watson, J Chem Phys 46 (1967) 1935.
[41] O.N. Ulenikov, H. Bürger, W. Jerzembeck, G.A. Onopenko, E.S. Bekhtereva, O.L. Petrunina, J. Mol. Struct. 599 (2001) 225.
[42] O.N. Ulenikov, E.S. Bekhtereva, S.V. Grebneva, H. Hollenstein, M. Quack, Phys. Chem. Chem. Phys. 7 (2005) 1142.
[43] O.N. Ulenikov, R.N. Tolchenov, M. Koivusaari, S. Alanko, R. Anttila, J. Mol. Spectrosc. 167 (1994) 109.
[44] S.-M. Hu, O.N. Ulenikov, G.A. Onopenko, E.S. Bekhtereva, S.-G. He, X.-H. Wang, H. Lin, Q.-S. Zhu, J. Mol. Spectrosc. 203 (2000) 228.
[45] J.-J. Zheng, O.N. Ulenikov, G.A. Onopenko, E.S. Bekhtereva, S.-G. He, X.-H. Wang, S.-M. Hu, H. Lin, Q.-S. Zhu, Mol. Phys. 99 (2001) 931.
[46] O.N. Ulenikov, S.-M. Hu, E.S. Bekhtereva, G.A. Onopenko, S.-G. He, X.-H. Wang, J.-J. Zheng, Q.-S. Zhu, J. Mol. Spectrosc. 210 (2001) 18.
[47] A.-W. Liu, O.N. Ulenikov, G.A. Onopenko, O.V. Gromova, E.S. Bekhtereva, L. Wan, L.-Y. Hao, S.-M. Hu, J.-M. Flaud, J. Mol. Spectrosc. 238 (2006) 23.
[48] O.N. Ulenikov, A.-W. Liu, E.S. Bekhtereva, O.V. Gromova, L.-Y. Hao, S.-M. Hu, J. Mol. Spectrosc. 226 (2004) 57.